

Fuel Properties of Oxymethylene Ethers with Terminating Groups from Methyl to Butyl

Stephen P. Lucas,[†] Fan Liang Chan,[†] Gina M. Fioroni,[‡] Thomas D. Foust,[‡]
Alayna Gilbert,[¶] Jon Luecke,[‡] Charles S. McEnally,[§] Justine John A.
Serdoncillo,^{||} Andrew J. Zdanowicz,[†] Junqing Zhu,[§] and Bret Windom^{*,†}

[†]*Department of Mechanical Engineering, Colorado State University, 1374 Campus
Delivery, Fort Collins, CO 80523-1374, United States*

[‡]*National Renewable Energy Laboratory, 15013 Denver W Pkwy, Golden, CO 80401,
United States*

[¶]*Department of Chemical and Biological Engineering, Colorado State University, 1370
Campus Delivery, Fort Collins, CO 80523-1370, United States*

[§]*Department of Chemical and Environmental Engineering, Yale University, 9 Hillhouse
Avenue, New Haven, CT 06520, United States of America*

^{||}*Department of Mechanical and Aerospace Engineering, Syracuse University, 223 Link
Hall, Syracuse, NY 13244, United States*

E-mail: Bret.Windom@colostate.edu

Abstract

Oxymethylene ethers (OMEs) have been studied as possible additives or replacements for diesel fuels. Typically, studies have considered only methyl-terminated OMEs. Recent structure-property relationship models suggest that extended-alkyl OMEs may provide improvements to many of the properties of methyl-terminated OMEs that make them less suitable as diesel fuel blendstocks. In this work, we describe the synthesis and characterization of 16 different OMEs with methyl, ethyl, propyl, butyl, isopropyl, and isobutyl terminating alkyl groups with varying oxymethylene chain length. Indicated Cetane Number, Lower Heating Value, Flash Point, Density, Viscosity, Vapor Pressure, and Oxidative Stability are tested via ASTM standard methods. Additionally, Water Solubility, Boiling Point, seal material compatibility, and sooting propensity (via the Yield Sooting Index) are measured for these fuels. For diesel compatibility, all tested OMEs except smaller methyl and ethyl OMEs, and the branched isopropyl OME, meet cetane number requirements. Extending the alkyl end group increases the heating value, but all OMEs, due to their oxygen content, have heating values less than diesel; despite this, all OMEs show significant reductions in soot production per unit heating value. Only the heaviest OMEs meet diesel viscosity requirements, and most are higher density than diesel. OMEs with larger alkyl groups show the highest stability under accelerated auto-oxidation conditions. Increases in alkyl group length cause order of magnitude reduction in water solubility, from hundreds of g/L for methyl terminated OMEs to hundreds of mg/L for butyl terminated OMEs. Limited seal material testing indicates that PEEK polymers are unaffected by OMEs; while extended alkyl groups may improve compatibility with FKM (Viton), other common elastomers (NBR, silicone) remain incompatible with all tested OMEs. Overall, it is found that methyl-terminated OMEs exhibit the most potential for soot reduction, but OMEs with larger propyl and butyl terminating alkyl groups show improved compatibility with existing diesel systems.

1 Introduction

2 Compression ignition (diesel) engines are currently the most common prime mover for
3 medium and heavy duty vehicles in the United States and around the world. Road freight
4 accounts for roughly half of diesel consumption globally,¹ with concurrent environmental
5 costs. In the US alone, medium and heavy duty vehicles account for approximately a quar-
6 ter of greenhouse gas (GHG) emissions, and more than half of nitrogen oxide (NO_x) and
7 particulate matter (PM) emissions.² As a result, there have been a number of attempts to
8 reduce various emissions from diesel engines; of note are US 2007 on-road and Tier 4 off-
9 road, and European Tier 1-6/I-VI, emissions regulations. US EPA on-road standards require
10 model year 2007 and newer vehicles produce less than 0.2 g/bhp-hr NO_x and 0.01 g/bhp-
11 hr PM emissions, while EU Tier 6/VI, which targets PM and NO_x emissions below 0.01
12 and 0.46 g/km respectively,³ has been adopted throughout the European Union (EU) and
13 India, and various other tiers have been adopted by other nations in Asia and Latin Amer-
14 ica.³ While the increasingly stringent regulations typically lead to equipment manufacturers
15 making improvements to engines and exhaust treatment systems, there are significant op-
16 portunities to reduce criteria pollutants and life cycle GHG emissions through development
17 of new fit-for-purpose sustainably derived fuels and blendstocks.

18 Sustainably derived ethers have previously been studied as blendstocks for diesel to re-
19 duce many of these emissions. Around the turn of the millennium, focus was given to
20 dimethyl ether as a diesel additive,⁴ and later, to oxymethylene ethers.⁵⁻⁸ Oxymethylene
21 ethers (OMEs), typically of the form R-O-(CH₂O)_n-R', have shown promise specifically in
22 the area of reduction of PM emissions, with some OME fuels exhibiting as much as 90% re-
23 duction in PM compared to traditional diesel fuel.^{7,8} Most studies have investigated OMEs
24 where R and R' are both methyl (CH₃) groups and n, or the number of oxymethylene
25 units, is either 1 or a range from 3-6 (often referred to polyoxymethylene dimethyl ethers).
26 Despite the significant reduction of PM, these methyl-terminated OMEs suffer from sev-
27 eral inferior properties to diesel fuel, including heating value, viscosity, seal compatibility,

28 and, for shorter oligomers, reactivity. For example, the simplest methyl-terminated OME,
29 dimethoxymethane (with only a single oxymethylene unit), has a Cetane Number (CN) of
30 28,⁶ well below diesel requirements, which range from as low as 40 in the United States
31 to 51 in the European Union.^{9,10} Most methyl-terminated OMEs have kinematic viscosities
32 less than 2 mm²/s, the minimum standard for diesel, and dimethoxymethane has the high-
33 est Lower Heating Value (LHV) of traditional OMEs at 23.3 MJ/kg, only slightly higher
34 than half that of typical diesel fuel.⁶ Several recent works have considered the effects of
35 methyl-terminated OMEs on various common seal materials, concluding that many common
36 elastomers used in fuel systems exhibit significantly higher OME absorption in comparison
37 to diesel fuel.^{8,11,12} Additionally, one recent work has included dibutoxymethane blended
38 with diesel in an exposure test of various thermoplastics and thermosets to diesel/additive
39 blends,¹³ and it was shown that as a blend with these hard polymers, there was little effect.

40 Recent work by Bartholet et al.¹⁴ developed models of various OME structures and sug-
41 gested that OMEs with non-methyl terminating alkyl groups may have superior properties
42 for blending with diesel, without sacrificing too much of the soot-reduction potential observed
43 for methyl-terminated OMEs. While the modeling results point to significant promise for
44 these OME variations as diesel fuel blendstocks, limited measured property data exists in
45 the literature for these molecules. Ethyl-terminated OMEs have received the most atten-
46 tion of these possible variations, with studies considering such details as physico-chemical
47 properties,⁶ engine performance,¹⁵ and even chemical kinetics.¹⁶⁻¹⁸ These works agree with
48 the trends found in Bartholet,¹⁴ wherein ethyl-terminated OMEs have improved heating val-
49 ues, higher viscosity, and continue to have acceptable autoignition properties. Additionally,
50 recent work by Drexler et al.¹⁹ has synthesized and characterized a number of symmetric
51 and asymmetric OMEs with extended and branched terminating alkyl groups, all with only
52 one oxymethylene unit. These OMEs are found to have comparable densities to diesel, and
53 improved diesel-relevant properties such as CN, flash point, and viscosity, when compared to
54 dimethoxymethane. In particular, Drexler shows that freeze points of extended-alkyl OMEs

55 are extremely low, in some cases below -100°C .¹⁹ These values indicate that for extended-
56 alkyl OMEs blended with diesel fuel, cold flow properties will be driven primarily by the
57 diesel components and are of minimal concern for blendstock selection, so we do not address
58 them further here. A past work by Murphy has shown that B-1-B has acceptable miscibility
59 with diesel.²⁰ Additional work by Arellano-Treviño et al.²¹ and An et al.²² has considered
60 the synthesis of, and measured some properties of, mixtures of butyl-terminated OMEs, but
61 neither made any attempt to isolate and characterize individual components of their synthe-
62 sis products. While these previous works demonstrate potential for improving the suitability
63 of OMEs for fuel use by altering the alkyl terminations, there has not been a systematic
64 study which varies both end group and oxymethylene chain length simultaneously to isolate
65 influences of each alteration on the fuel properties.

66 Synthesis of OMEs is a well-studied process and thus there is a strong basis of literature
67 for methods to synthesize new OMEs for study and consideration as future fuel blend-
68 stocks. In general, OMEs are synthesized through the formation of dimethoxymethane from
69 methanol via various methods such as acetalization,⁵ conversion of dimethyl ether,^{23,24} and
70 recently through dehydrogenation,²⁵ followed by elongation (i.e. increasing of the number
71 of oxymethylene units) via a formaldehyde source such as paraformaldehyde or trioxane, as
72 reviewed by Baranowski.²⁶ Methanol and higher alcohols can be produced from biological
73 sources,^{27,28} and formaldehyde production from methanol is well documented²⁹ and one of
74 the most common industrial production methods – thus, it is reasonable to conclude that
75 processes to formulate these OMEs using bio-sourced materials are possible with current
76 technologies.

77 In this work, 16 different OMEs with methyl, ethyl, propyl, butyl, isopropyl, and isobutyl
78 terminating alkyl groups are synthesized and characterized, in order to provide a broad
79 reference of relevant properties so that future combustion and engine studies may more
80 easily select a particular OME (or mix thereof) based upon the desired balance of properties
81 important in fuel handling, engine performance, and emissions, including improved soot

82 reduction. Of these 16, 10 have been studied before for fuel properties,^{6,19,30,31} although not
83 all tests performed here (e.g. water solubility, oxidative stability) have been performed for
84 all of these. The remaining six OMEs have not, to our knowledge, been studied for fuel
85 properties. Recommendations are provided based upon these results for the ideal OME for
86 various goals such as maximal soot reduction or best overall compatibility with diesel fuel.

87 **Nomenclature and Structures**

88 Numerous abbreviations for OMEs have been used in literature, such as OME, POME,
89 PODE, OMDME, etc. Given the variety of OMEs tested here, this work uses a short-
90 hand method to highlight the specifics of each molecule, referring to the OMEs using the
91 abbreviation X - n - Y , where X and Y refer to the terminating alkyl groups – M =Methyl,
92 E =Ethyl, P =Propyl, B =Butyl, iP =isoPropyl, and iB =isoButyl – and n refers to the num-
93 ber of oxymethylene units in the central chain. Note that the total number of oxygen atoms
94 in these OMEs is $n+1$ as there is always one additional oxygen which is not a member of an
95 oxymethylene unit.

96 As an example of this nomenclature, Fig. 1 shows butoxymethoxymethoxybutane, which
97 is here termed B-2-B. It is possible to produce non-symmetric OMEs where X and Y are
98 not the same; indeed, some of these molecules arise from the trans-acetalization reactions
99 used in Arellano-Treviño’s recent work²¹ and make up part of the resultant tested mixture.
100 However, this work focuses on symmetric OMEs to highlight the trends in properties from
101 either alkyl group effects or chain length effects; asymmetric OMEs are beyond the intended
102 scope of this work. Specifically for the iso-OMEs, iP -1- iP and iB -1- iB , the oxygen is attached
103 at the same location as the hydroxyl group of the corresponding alcohol; for clarity, these
104 structures are provided below in Figs. 2 and 3.

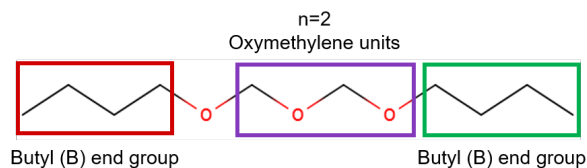


Figure 1: Example OME structure – B-2-B

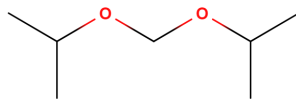


Figure 2: iP-1-iP

105 Methods

106 Fuels Used

107 The OMEs tested in this work are a combination of commercially available and synthesized
 108 in-house. All methyl-terminated OMEs were acquired commercially. M-1-M was purchased
 109 from Fisher Scientific and Sigma Aldrich, purity >98%. M-2-M was purchased from AstaTech
 110 Inc., purity >97%. M-3-M through M-5-M were acquired as a mixture from ASG Analytik-
 111 Service GmbH, and was distilled in-house to purities >95%. E-1-E was purchased from
 112 Fisher Scientific and Sigma Aldrich, purity >98%. P-1-P was provided as a sample by
 113 Lambiotte & Cie, purity >97%. B-1-B was purchased from Fisher Scientific and Sigma
 114 Aldrich, purity >98%. E-2-E, E-3-E, P-2-P, P-3-P, B-2-B, and B-3-B were synthesized via
 115 elongation of the appropriate X-1-X with trioxane over Amberlyst 15 catalyst²⁶ and distilled
 116 to purity >95%. iP-1-iP and iB-1-iB were synthesized from trioxane and the corresponding
 117 iso-alcohol over Amberlyst 15 catalyst and distilled to purity >95%. For the extended OMEs,
 118 typical impurities consisted of small amounts of the oligomers with one more and one fewer

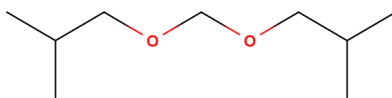


Figure 3: iB-1-iB

119 oxymethylene units.

120 Table 1 is provided below for CAS numbers of OMEs where these have been registered;
121 additionally, basic properties such as molecular weight (MW) and oxygen content by mass
122 are provided.

Table 1: CAS Number, Molecular Weight, and Oxygen Content of Tested OMEs

OME	CAS #	MW	Oxygen Mass%
M-1-M	109-87-5	76.09	42.05
M-2-M	628-90-0	106.12	45.23
M-3-M	13353-03-2	136.15	47.01
M-4-M	13352-75-5	166.17	48.14
M-5-M	13352-76-6	196.2	48.93
E-1-E	462-95-3	104.15	30.72
E-2-E	5648-29-3	134.17	35.77
E-3-E	4431-82-7	164.2	38.98
P-1-P	505-84-0	132.2	24.21
P-2-P	Not registered	162.23	29.59
P-3-P	4478-22-2	192.25	33.29
B-1-B	2568-90-3	160.25	19.97
B-2-B	Not registered	190.28	25.23
B-3-B	Not registered	220.31	29.05
iP-1-iP	2568-89-0	132.2	24.21
iB-1-iB	2568-91-4	160.25	19.97

123 **Testing Methods**

124 In this work, several properties were measured for the matrix of OME variations. For some
125 properties, ASTM standard methods were available, however, a number did not have ASTM

126 standard methods available, or the available methods were not designed to handle the range
127 of values encountered in the testing. As much as possible, each test was attempted to be
128 performed on all of the desired molecules; however, due to limited quantities of some of the
129 more difficult molecules to isolate, some tests were performed only on a subset in order to
130 show the likely trends.

131 For the ASTM standard methods, the following tests were performed:

- 132 • Indicated Cetane Number (ICN), ASTM D8183.³² This method is certified in the range
133 of $35 < ICN < 85$, and while it can measure results outside this range, the accuracy is
134 not guaranteed in the standard. Work by Abel et al. has shown that this method has
135 good agreement with other CN measurement standards in normal diesel ranges, and
136 that only for extremely high or low reactivity fuels do the several common methods
137 start to diverge.³³ These tests were performed in a Seta Analytics Advanced Fuel
138 Ignition Delay Analyzer (AFIDA).
- 139 • Lower Heating Value (LHV), ASTM D240.³⁴ Note that this method directly measures
140 the higher heating value; LHV can be calculated via stoichiometry and the known heat
141 of vaporization of water. These tests were performed in an IKA C200 calorimeter.
- 142 • Flash Point (FP), ASTM D93A.³⁵ These tests were performed in an Anton-Paar PMA4
143 closed-cup flash point tester. This method was not able to process flash points below
144 ambient conditions, and so some lighter OMEs could not be safely tested.
- 145 • Density and Viscosity (ρ and ν), ASTM D7042.³⁶ Measurements were conducted over
146 a range of temperatures from 20-100°C where possible. These tests were performed in
147 an Anton-Paar SVM-3000 viscometer.
- 148 • Vapor Pressure, ASTM D6378.³⁷ From this data, a curve-fit was applied to calculate
149 Antoine equation coefficients. These tests were performed in a Grabner Instruments
150 VPXpert-L vapor pressure tester.

151 • Oxidative Stability, ASTM D7545.³⁸ These tests were performed in a Petrotest PetroOXY
152 device as 20 vol.% blends in tridecane to simulate likely blending conditions.

153 For non-ASTM test methods, the following tests were performed:

154 • Yield Sooting Index (YSI)

155 • Water Solubility (WS)

156 • Boiling Point (BP)

157 • Seal material compatibility

158 YSI characterizes the sooting propensity of a fuel based on the amount of soot formed
159 when the test compound is doped into the fuel of a methane/air nonpremixed flame.^{39,40}
160 The raw soot concentrations are rescaled relative to two endpoint species to produce an
161 index analogous to an octane number or a cetane number. For the B-n-B OMEs, the stan-
162 dard methodology was used: dopant mole fraction = 1000 ppm, upper endpoint = toluene
163 (YSI \equiv 170.9), and lower endpoint = *n*-heptane (YSI \equiv 36.0).⁴¹ However, these parameters
164 were changed for the other OMEs to accommodate their very low sooting tendencies.⁴² In
165 particular, the dopant mole fraction was raised to 3000 ppm to increase the absolute soot
166 concentrations, *n*-heptane was switched to the upper endpoint, and water (YSI \equiv 0.0) was
167 adopted as the lower endpoint to minimize extrapolation of the measured YSIs outside of
168 the endpoint range.

169 Water solubility was measured in a HP 5890 Series II gas chromatograph with a flame
170 ionization detector (GC-FID) in a 30 m Restek Rtx-Wax column, 0.25 mm diameter with 0.25
171 μ m film. As water cannot be accurately measured in a GC-FID device, a relative response
172 ratio (RRR) method was used. The target OME was blended with 99% ethanol (*n*-propanol
173 was used for the iP-1-iP case due to simultaneous elution of ethanol and iP-1-iP) at known
174 masses after drying over MS4Å molecular sieves, and the responses recorded:

$$RRR = \frac{area_{ethanol}/mass_{ethanol}}{area_{OME}/mass_{OME}} \quad (1)$$

175 From here, the OMEs were blended with Type I deionized water in individual vials (five
176 samples per OME), shaken vigorously, and left to diffuse to equilibrium for 72 hours. The
177 water layer was extracted, added to clean vials and the mass recorded, then a known mass of
178 ethanol added. This mixture was tested in the GC-FID, and from the known mass of ethanol
179 and measured response areas, the mass of OME can be calculated. From here, the mass of
180 water is the remainder of the measured mass of OME/water blend, and water solubility in
181 g/g is calculated:

$$mass_{OME} = RRR * \frac{area_{OME}}{area_{ethanol}/mass_{ethanol}} \quad (2)$$

182 This method provides good coefficient of variance (CoV, <5% for most samples), but the
183 very low solubility of butyl-terminated OMEs resulted in higher CoV (approximately 15%)
184 as the samples used masses of OME and ethanol only one order of magnitude higher than
185 the resolution of the balance used.

186 Boiling points were not measured directly, but calculated from reduced pressure boiling
187 points during purification. The reduced pressures were converted to atmospheric equivalents
188 using the Atmospheric Equivalent Temperature calculation described in ASTM D1160.⁴³

189 Material compatibility was tested on small (approximately 1 mm x 10 mm x 25 mm)
190 coupons of the selected materials submerged in the OME fuels. Four representative materials
191 were tested – silicone rubber, nitrile rubber (NBR), and fluoroelastomer (FKM), which
192 represent a number of common flexible seal materials, and poly-ether ether ketone (PEEK),
193 a hard polymer sometimes used as a valve seat material. Polytetrafluoroethylene (PTFE)
194 is one of the most common chemical-resistant hard sealing and valve seat materials, but
195 it has been shown in literature to be resistant to OMEs⁸ and so PEEK was selected as
196 an interesting alternate material. Two coupons of each material had the mass taken before
197 immersion, then at 24, 48, 72, and 144 hours of exposure to test for fuel absorption, and then
198 again after drying in a fume hood for 24 and 48 hours to test for any permanent damage.
199 When possible, the OME sample was unchanged, but some of the volatile OMEs required
200 replenishing during the measurements to ensure the samples remained fully submerged.

201 Results and Discussion

202 Indicated Cetane Number

203 ICN was measured as the average of two tests due to the larger quantity of fuel required
204 (approximately 40 mL per test). For all fuels, 2000 ppm of Infineum R655, a lubricity
205 additive, was mixed with the fuel to ensure proper injector operation. Tests with P-1-P and
206 B-1-B without the lubricity additive showed negligible (<0.3) change in ICN due to this
207 additive. The average deviation from the mean is 0.55%, with iP-1-iP having the highest
208 difference between its two measurements at 1.5%. The measured values are presented in
209 Table 2. On-road diesel fuels in the US are typically $\text{ICN} > 40$, with Texas requiring $\text{ICN} > 48$
210 and California requiring $\text{ICN} > 53$. The EU requires $\text{ICN} > 51$.

Table 2: Indicated Cetane Number of various OMEs

End Group	Number of CH ₂ O Units				
	1	2	3	4	5
Methyl	25.6	56.1	64.0	71.1	85.2
Ethyl	41.1	60.3	59.4		
Propyl	53.2	59.3	66.1		
Butyl	76.3	76.9	76.0		
Isopropyl	11.2				
Isobutyl	53.2				
Typical Diesel	>40				

211 Based upon these criteria, it is found that M-2-M and longer methyl OMEs, and all
212 ethyl, propyl (except iP-1-iP), and butyl OMEs meet the minimum US requirements, and
213 for maximum compatibility, M-2-M and higher, E-2-E and E-3-E, and all propyl (except iP-
214 1-iP) and butyl OMEs are the best candidates. Larger alkyl groups are less sensitive to the
215 length of the oxymethylene chain on ICN, up to the point where the ICN of butyl-terminated

216 OMEs appears entirely independent of the number of oxymethylene units. The kinetics of
217 extended-alkyl OMEs are a new frontier in combustion chemistry; some recent works by
218 Kroger et al.,¹⁶ Jacobs et al.,¹⁸ and Li et al.¹⁷ have considered the kinetics of E-1-E, but no
219 detailed chemical studies of larger extended-alkyl OMEs have been published. Recent work
220 by the authors⁴⁴ considers ignition behavior of E-1-E, E-2-E, P-1-P, and iP-1-iP in a rapid
221 compression machine, wherein it is hypothesized that the additional sites available for RO₂
222 pathways on the longer alkyl groups such as propyl have significant effects on ignition, which
223 may cause the decreased effect of chain length as alkyl groups are extended. Understanding
224 the full causes of these ignition behaviors will require significant future study in fundamental
225 theory and experiments.

226 Of particular note are the behaviors of the iso-OMEs, iP-1-iP and iB-1-iB. These have
227 significantly lower ICN than their linear counterparts P-1-P and B-1-B, by 79% and 30%
228 respectively. This is not an entirely unexpected result; for example, *n*-octane has a CN
229 of approximately 65 (depending on the exact measurement method), while its branched
230 counterpart iso-octane has CN approximately 17.⁴⁵ While detailed chemical mechanisms
231 have not been developed for any propyl- or butyl-terminated OMEs, work on methyl- and
232 ethyl-terminated OMEs indicates that RO₂ chemistry remains an important step in the
233 ignition of these fuels,^{16–18,44} and thus similar effects on inhibition of RO₂ pathways via
234 branched structures are to be expected and warrant further investigation. While ICN cannot
235 be directly converted to either form of octane number (RON or MON), it is clear that many
236 fuels with high octane numbers have low cetane numbers; the ICN of iP-1-iP is similar to
237 that of iso-octane, and this may warrant investigation of iP-1-iP as a potential gasoline,
238 rather than diesel, additive.

239 In the corrigendum to their 2016 analysis of M-n-M and E-n-E OMEs, Lautenschütz et al.
240 review cetane numbers, also using an AFIDA device.⁶ We find lower ICN for all comparable
241 OMEs than Lautenschütz, with an average difference of 13% lower ICN; the least difference
242 is in the E-2-E measurement (4.5% lower) and the highest in M-2-M (21% lower). Drexler

243 et. al.¹⁹ tested E-1-E, P-1-P, and B-1-B in an AFIDA; we find similar results to this work,
244 where the highest difference is a 3.2% higher ICN for P-1-P. In either case, the conclusions
245 are similar – most OMEs other than M-1-M, and in some jurisdictions E-1-E, meet diesel
246 requirements for reactivity.

247 In the literature, neat OMEs as well as OMEs blended with diesel fuel have been tested.⁷
248 Here ICNs were measured for a representative high-ICN OME, B-1-B, blended volumetrically
249 with a certified diesel, ICN=40.7, in increments of 10 volume % (Fig. 4). Due to the similar
250 densities of B-1-B and diesel, this is essentially equivalent to a mass ratio blend as well. It
251 is observed that the ICN of the mixture is nonlinear with volumetric blending; the presence
252 of B-1-B shows an antagonistic effect on mixture ICN resulting in a lower ICN than would
253 be predicted by linear blending rules; this is in agreement with existing literature on ether
254 blending effects in distillate fuels.⁴⁶ The maximum deviation from the linear blending rule is
255 6.3%, indicating that while the presence of the ether has some negative effect, it is insufficient
256 to overcome the ICN benefit of the high-reactivity OME.

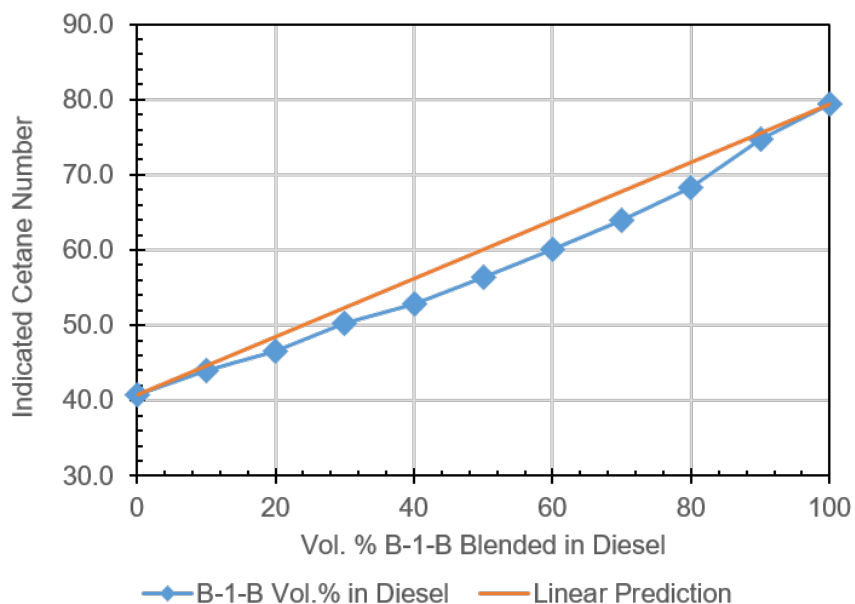


Figure 4: Effect of varying B-1-B blending ratio in diesel (ICN=40.7) on ICN of mixture, compared with a linear blending assumption.

257 **Lower Heating Value**

258 LHV was not measured directly; the calorimeter used (IKA C200) combusts a known mass
 259 fuel sample in an oxygen environment and measures the change in temperature of a water
 260 bath to determine energy released. As the water formed from combustion will condense
 261 when cooled, this method measures the higher heating value (HHV). For engine operation,
 262 LHV is the more applicable measurement as the combustion chamber is maintained at high
 263 temperature with very short dwell times, so under typical operation none of the latent heat
 264 of the water vapor will be released. Thus, HHV is converted to LHV via the assumption
 265 of complete combustion and subtraction of the latent heat of the produced water mass; the
 266 results of this analysis are presented in Table 3.

267 ASTM D975 and EN590 diesel standards do not specify a minimum acceptable value for
 268 LHV or HHV of diesel; however, typical diesels have $LHV > 42$ MJ/kg,⁴⁷ and while biodiesel
 269 LHV will depend in part on the oxygen content, some traditional biodiesels have been found
 270 to have LHV between 37 and 40 MJ/kg.^{47,48} Synthetic diesels from processes such as Fischer-
 271 Tropsch or hydrotreatment of bio-oils may have much higher LHVs, up to 49 MJ/kg.⁴⁹ The
 272 high oxygen content of OMEs results in significantly lower LHVs than traditional diesels, a
 273 weakness noted in prior work.⁶ OMEs with extended alkyl groups reduce the oxygen:carbon
 274 ratio and thus should produce higher LHVs, and one would further expect longer oxymethy-
 275 lene chain OMEs to produce lower LHV than their shorter counterparts.

Table 3: Lower Heating Value of various OMEs [MJ/kg]

End Group	Number of CH ₂ O Units				
	1	2	3	4	5
Methyl	23.2	21.0	20.0	19.3	18.8
Ethyl	28.8	25.9	24.1		
Propyl	32.0	29.0	27.0		
Butyl	34.1	31.2	29.2		

Isopropyl	31.4
Isobutyl	33.7
Typical Diesel	>42

276 These results are consistent with expectations; higher alkyl groups produce higher LHV,
 277 and longer oxymethylene chains produce lower LHV. There is a diminishing effect on the
 278 reduction in LHV per oxymethylene unit as the ratio of oxygen:carbon approaches unity with
 279 longer chains. The iso-OMEs diverge again from their linear counterparts, but only slightly.
 280 This is also consistent with alkane behavior, where LHV of branched molecules is slightly
 281 reduced in comparison to linear variants.⁵⁰ The reported values here for M-n-M, E-n-E, P-
 282 1-P, and B-1-B are in good agreement with literature,^{6,19,30,31} with a maximum difference of
 283 4.9% higher LHV reported here for E-1-E compared to measurements from Drexler et al.¹⁹
 284 In our data, an average coefficient of variance (CoV) of 1.2% is found, with M-1-M showing
 285 the highest CoV of 4.6%.

286 None of the tested OMEs show what could be considered “high” LHV; even the highest
 287 tested value, for B-1-B, is still approximately 3 MJ/kg less than many typical biodiesels.⁴⁷
 288 For maximizing energy content, we recommend usage of OMEs with as long of terminating
 289 alkyl groups as other requirements may permit.

290 Yield Sooting Index

291 Smoke point measurements by Tan et al.⁵¹ show that methyl-terminated OMEs, which con-
 292 tain no carbon-carbon bonds, have negligible sooting tendencies compared to conventional
 293 diesel fuel. In contrast, extended alkyl OMEs do contain carbon-carbon bonds, so they would
 294 be expected to have higher sooting tendencies, which diminishes one of the most important
 295 attributes of OMEs as alternative diesel fuels. One of the main objectives of this work is
 296 to quantify the trade-off between sooting tendency and the desirable properties of extended
 297 alkyl OMEs (e.g., higher LHV, lower water solubility). The smoke points of the OMEs are

298 outside the measurement limits of the ASTM D1322 standard and cannot be determined
 299 directly.⁵² However, the YSI approach used in this study has a much wider dynamic range
 300 and values could be measured for all the neat OMEs.

Table 4: Yield Sooting Index of various OMEs

End Group	Number of CH ₂ O Units				
	1	2	3	4	5
Methyl	6.6	5.2	0.5	-2.5	-4.8
Ethyl	15.5	13.8	11.9		
Propyl	30.8	25.5	21.3		
Butyl	46.0	42.7	37.8		
Isopropyl	38.4				
Isobutyl	52.2				
Typical Diesel	>200				

Table 5: YSI/LHV of various OMEs [1/(MJ/kg)]

End Group	Number of CH ₂ O Units				
	1	2	3	4	5
Methyl	0.284	0.248	0.025	-0.130	-0.255
Ethyl	0.538	0.533	0.494		
Propyl	0.963	0.879	0.789		
Butyl	1.35	1.37	1.29		
Isopropyl	1.22				
Isobutyl	1.55				
Typical Diesel	~4.8				

301 Table 4 lists the measured YSIs and Table 5 lists the ratios of the YSIs to the LHV
 302 reported in the prior section. YSI uncertainty is +/- 7%. YSI quantifies the amount of

303 soot formed per mole of fuel, whereas YSI/LHV indicates the amount of soot produced per
 304 unit of fuel energy, which is the more engine-relevant quantity. The YSIs demonstrate that
 305 all the OMEs significantly reduce soot compared to diesel fuel: the sootiest OME, iB-1-iB,
 306 decreases it by a factor of 3.8 while the least sooty OMEs, M-4-M and M-5-M, decrease it by
 307 an effectively infinite ratio since they have negative YSIs. These negative YSIs are discussed
 308 in more detail elsewhere;⁴² in short, they occur because M-4-M and M-5-M produce virtually
 309 no soot and instead decompose to large quantities of formaldehyde (CH_2O), which suppresses
 310 soot formation from the methane background fuel in the YSI flames to a total soot fraction
 311 below that observed in the zero YSI case. The results in Table 5 show that the reductions in
 312 YSI/LHV are smaller, but still significant. For example, whereas iB-1-iB reduces YSI by a
 313 factor of 3.8, it reduces YSI/LHV by a factor of 3.1. This observation demonstrates that the
 314 OMEs reduce soot even when accounting for the larger amount of fuel required to produce
 315 a given amount of energy.

316 **Flash Point**

317 Flash point (FP) is an important factor in the safety of handling fuels; while gasolines
 318 typically have FP well below ambient and are treated as flammable liquids, diesel fuels
 319 typically have FP $>52^\circ\text{C}$ ($>55^\circ\text{C}$ in the EU) and are classified as combustible liquids.⁵³ As
 320 documented by Härtl et al. and Lautenschütz et al.,^{6,30} smaller OMEs such as M-1-M and
 321 E-1-E have FP below or close to this requirement, but the most commonly studied OMEs
 322 (M-3-M and higher) will meet this requirement.

Table 6: Flash Point of various OMEs [$^\circ\text{C}$]

End Group	Number of CH_2O Units				
	1	2	3	4	5
Methyl	$<20^{\text{a}}$	$<20^{\text{a}}$	56.4	85.6	116
Ethyl	$<20^{\text{a}}$	35.5	69.4		

Propyl	31.7	66.5	91.0
Butyl	58.6	89.6	114
Isopropyl	21.3		
Isobutyl	49.4		
Typical Diesel	>52		

^aFlash point too low to safely test in PMA4

323 As shown in Table 6, FP appears to be a significant weakness in compatibility of OMEs
324 with diesel; about half (M-3-M and higher, E-3-E, P-2-P and higher, and B-1-B and higher)
325 meet this requirement, while others do not. Our measurements have an average coefficient
326 of variance (CoV) of 0.98%, with B-1-B showing the highest CoV of 1.8%, for five tests
327 performed for each fuel. The reported values for M-n-M and E-n-E are in good agreement
328 with Lautenschütz’s work, with a maximum deviation of <1% higher for M-3-M.⁶ We also
329 find comparable FP to Drexler et al.¹⁹ for P-1-P and B-1-B, with <1% difference. Some of
330 these fuels had FP too low to safely test in the PMA4 device, which is not natively equipped
331 to test FP below ambient temperatures, and while some cooling of the test cup is possible, a
332 different device with native cooling capability may be required for testing of low-FP OMEs;
333 we note that Lautenschütz et al. report FP values for M-1-M and E-1-E of -32°C and -5°C
334 respectively⁶ and Deutsch et al. report a FP of 16°C for M-2-M,³¹ below the safe testing
335 limits of the methods used here.

336 **Density and Viscosity**

337 Physical properties of the liquid fuel will have significant effects on the behavior of the spray
338 in the fuel injector for a CI engine; the influential work of Lefebvre on sprays indicate that
339 ρ and ν are of high importance for spray development.⁵⁴ The effect of biodiesels on the
340 performance of CI engine injectors has been a matter of concern due to typically higher
341 ρ and ν ; as reviewed by Algayyim et al., many studies have been conducted which find

342 that typical biodiesels produce sprays with greater penetration and larger diameter droplets,
 343 hindering evaporation due to lower area:volume ratios.⁵⁵ Further, some work suggests that
 344 larger droplets may increase soot formation.⁵⁶ CI engines are designed around combustion of
 345 a particular ideal fuel spray, so rather than preferring some minimum (e.g. YSI) or maximum
 346 (e.g. LHV), the ideal OME for diesel blending will match as closely as possible to typical
 347 diesel values. We present density of the OMEs at 20°C in Table 7, and the viscosity at 40°C
 348 in Table 8 below.

Table 7: Density at 20°C of various OMEs [g/mL]

End Group	Number of CH ₂ O Units				
	1	2	3	4	5
Methyl	0.860	0.992	1.03	1.07	1.10
Ethyl	0.829	0.912	0.971		
Propyl	0.834	0.900	0.948		
Butyl	0.837	0.888	0.931		
Isopropyl	0.818				
Isobutyl	0.824				
Typical Diesel	0.84-0.87				

Table 8: Kinematic Viscosity at 40°C of various OMEs [mm²/s]

End Group	Number of CH ₂ O Units				
	1	2	3	4	5
Methyl	n/a ^b	0.617	0.876	1.32	1.98
Ethyl	0.346	0.652	0.963		
Propyl	0.644	0.949	1.39		
Butyl	0.945	1.32	1.85		
Isopropyl	0.515				

Isobutyl	0.904
Typical Diesel	2.0-3.2

^bAt lab ambient pressure (84 kPa), M-1-M will boil at approximately 37°C, so no density or viscosity at 40°C can be measured without a device to maintain the viscometer above ambient pressure

349 None of the OMEs tested match perfectly with typical diesel for ρ except M-1-M; however,
350 all of the n=1 and n=2 OMEs are very close to diesel and may be good substitutes in this
351 respect. Longer oxymethylene chains produce higher ρ due to higher oxygen content, which
352 helps offset some LHV losses by allowing for more fuel mass per unit volume. Only two
353 tested OMEs, M-5-M and B-3-B, even approached the ν values typically seen in diesels,
354 with most being less than half that of the minimum diesel ν . The average CoV for ρ and ν
355 measurements was less than 0.1% for 3 tests per fuel.

356 In comparison with literature, we find nearly identical ρ measurements to Lautenschütz⁶
357 and Drexler,¹⁹ with the largest observed difference as a 1.5% higher ρ for M-2-M.⁶ For
358 ν , Lautenschütz et al. measure ν at 25 °C and Drexler et al. measure at 20 °C, while
359 Deutsch et al. measure at 40 °C, as reported in Table 8 above. We find good agreement
360 with Deutsch et al. for all values except M-2-M, where we observe a 9.2% higher ν . A
361 temperature sweep was performed for ρ and ν (Figs. 5-8) with a step of 10°C, so to compare
362 with Lautenschütz et al. we take an average of our 20°C and 30°C values. Acknowledging
363 that ν is nonlinear with temperature, and thus some small error is to be expected from this
364 approximation, we nonetheless find good agreement except for M-1-M and E-1-E, where we
365 observed significantly (16% and 19% respectively) lower ν than Lautenschütz et al. For E-
366 1-E, P-1-P, and B-1-B, we find a 15% lower ν for E-1-E than Drexler et al.,¹⁹ but find good
367 agreement (within 5%) for the remaining fuels.

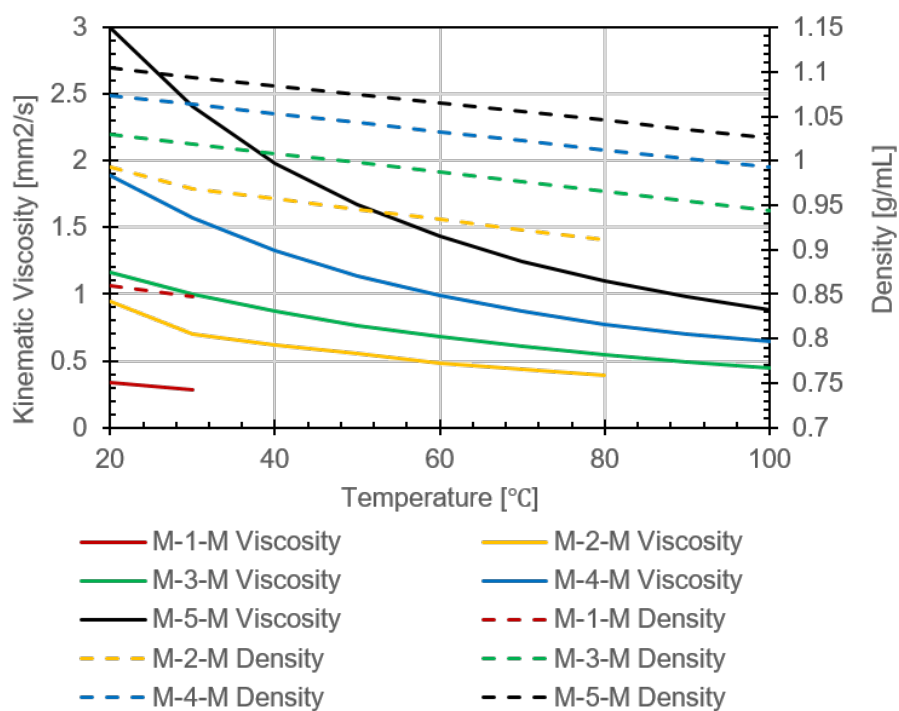


Figure 5: Viscosity and density curves of M-n-M OMEs between 20°C and 100°C

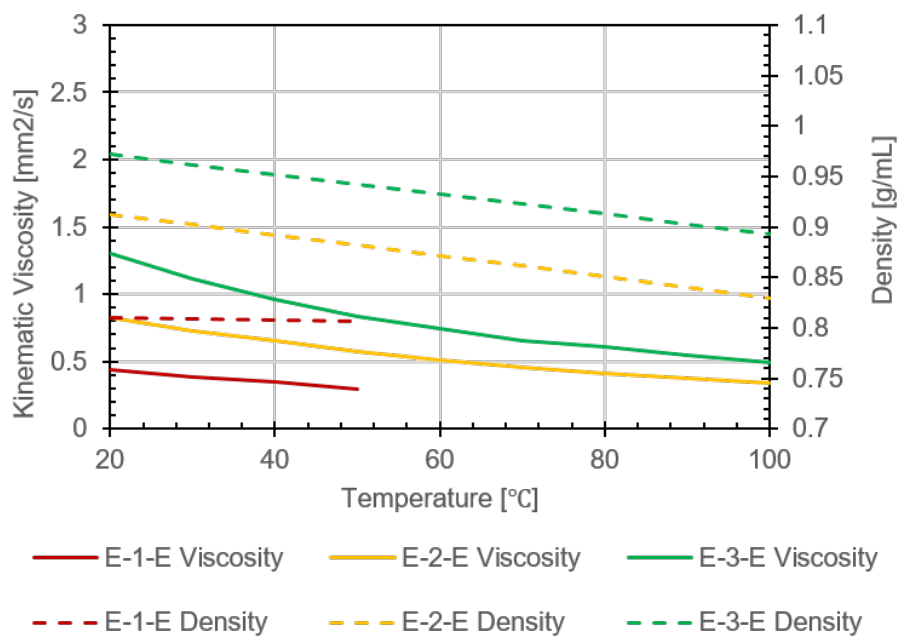


Figure 6: Viscosity and density curves of E-n-E OMEs between 20°C and 100°C

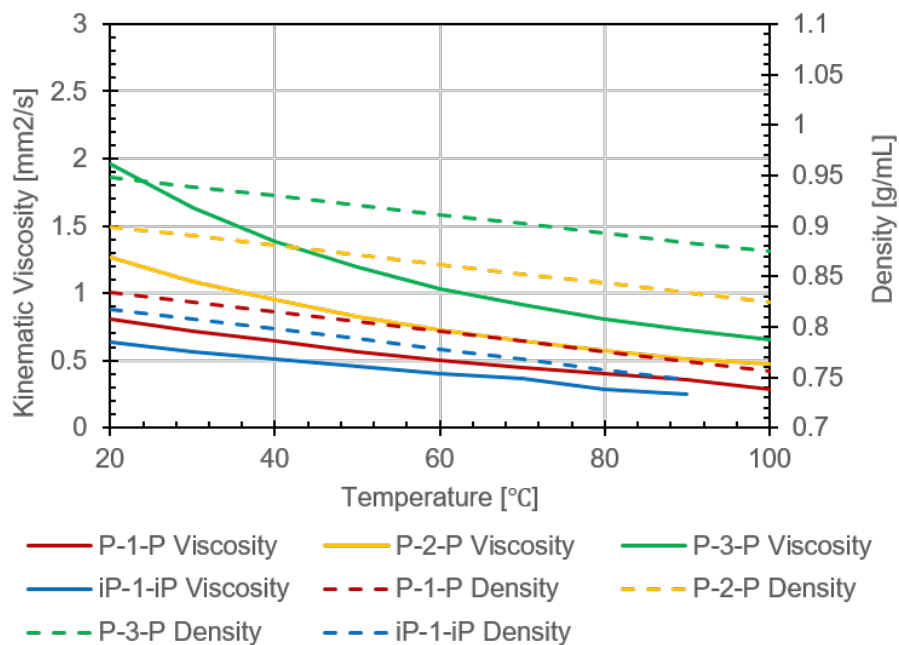


Figure 7: Viscosity and density curves of P-n-P and iP-1-iP OMEs between 20°C and 100°C

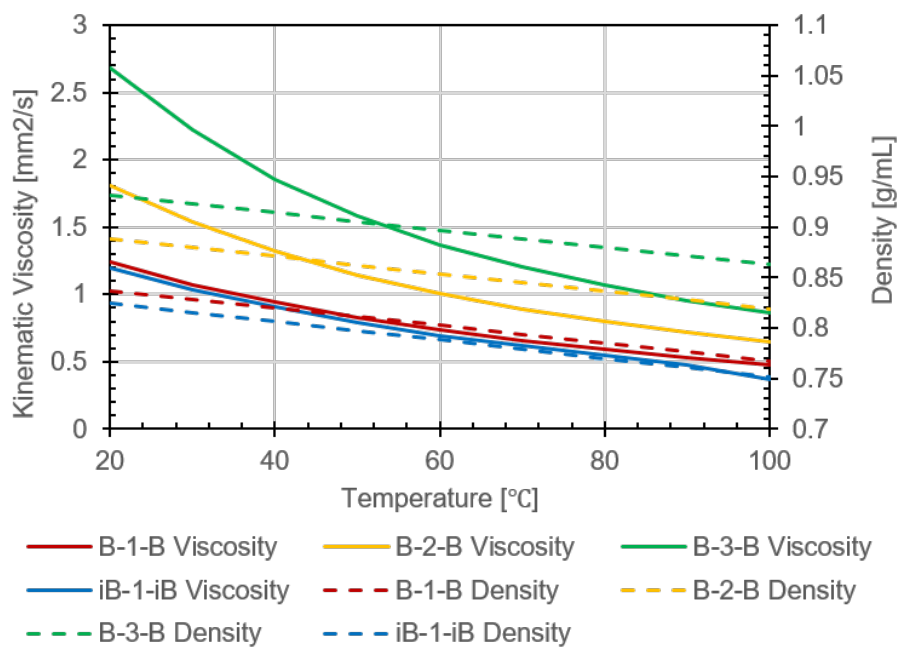


Figure 8: Viscosity and density curves of B-n-B and iB-1-iB OMEs between 20°C and 100°C

368 **Vapor Pressure**

369 A subset of the OMEs were tested for vapor pressure, however, due to high fuel volume
 370 requirements not all were tested. The tested OMEs were M-1-M, M-3-M, M-4-M, M-5-M,
 371 E-1-E, P-1-P, and B-1-B. Antoine equation (Eq. 3) parameters were calculated for these
 372 OMEs and are presented below; M-1-M and E-1-E have Antoine coefficients provided in the
 373 NIST Webbook^{57,58} and produce curves within 5% of our calculated values. The average
 374 CoV for five tests per fuel was 5.5%, driven primarily by exceptionally high CoV (29%)
 375 for M-5-M (the average CoV for the other tests, excluding M-5-M, was a more reasonable
 376 1.8%). Generally, CoV increased with decreasing volatility. Due to limits of the testing
 377 device and the fuels, different temperature ranges were tested, up to either just below the
 378 boiling temperature or the device maximum temperature (120°C), and starting at 0°C or a
 379 temperature providing above 5 mbar vapor pressure (to prevent damage to the machine due
 380 to low vacuum). Coefficients are reported as calculated from the curve fit, but we note that
 381 the measured values from which these are produced are accurate to 3 significant figures and
 382 calculated values from these should be treated as such.

$$\log_{10}(P_{vap}) = A - \frac{B}{C + T} \tag{3}$$

Table 9: Antoine equation coefficients for some OMEs [bar, K]

Fuel	Temp Range	A	B	C
	Tested [°C]			
M-1-M	0-35	3.881	991.89	-59.23
E-1-E	0-80	3.995	1201.2	-59.07
P-1-P	20-120	4.762	1920.2	1.598
B-1-B	30-120	3.911	1882.5	32.66
M-3-M	20-120	4.246	1629.4	-24.69

M-4-M	30-120	4.309	2130.2	39.43
M-5-M	50-120	4.142	2301.4	49.54

383 The vapor pressure of diesel will vary with the various volatile components, so several
 384 common alkanes are shown on the plot below (Fig. 9) using Antoine parameters from
 385 NIST⁵⁹⁻⁶¹ to provide a point of reference.

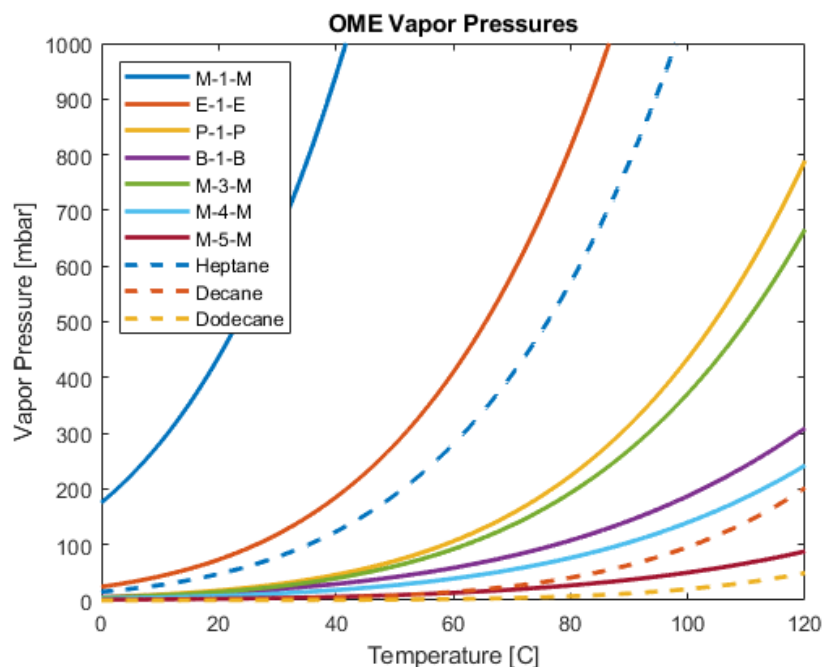


Figure 9: Antoine curves of OME vapor pressure, from calculated Antoine coefficients, compared to some typical alkanes (see Table 9)

386 Oxidative Stability

387 The most common test for oxidative stability of biodiesels is the Rancimat test (EN 15751).
 388 This test was attempted for oxidative stability, however, the nature of the method caused
 389 significant difficulties and was determined to be ineffective for testing OMEs. First and most
 390 relevant, the Rancimat test is by nature an open-system test. The oxidation is accelerated by
 391 pumping air through a heated fuel sample, and the volatiles (nominally acids) are collected

392 in water, with changes in the conductivity of the water indicating the presence of acids
393 formed from auto-oxidation. As a result of heating to the test temperature of 110°C and
394 simultaneously enforcing a gas flow, many of the OMEs will rapidly vaporize or even boil
395 and be lost – further, as will be discussed in a later section, the water solubility of many
396 OMEs is very high and vapors will contaminate the measuring water. The second problem
397 is the nature of the test, which uses conductivity change of a water sample as a proxy for
398 oxidation. This has been shown to work well for fatty-acid methyl ester biofuels,⁶² but it was
399 not clear prior to the tests whether the auto-oxidation products of an OME will necessarily
400 ionize or otherwise change the conductivity of the measuring water.

401 As a result of these difficulties, a different test was used. The Petro-Oxy testing device is
402 often used for gasoline and gasoline additives,⁶³ which makes it more suitable for the OMEs,
403 some which have been shown to have higher volatility. Additionally, it is a closed-system
404 measurement, preventing the vapor losses seen in some initial failed attempts to use the
405 Rancimat method. The Petro-Oxy device subjects a small (5 mL) sample of the fuel to 140
406 °C under 7 bar of oxygen, and measures the induction time as defined by the time to a 10%
407 reduction from the maximum pressure of the test.³⁸ Some past work has applied this method
408 to biodiesels in comparison with the Rancimat method and determined minimum equivalent
409 Petro-Oxy induction times,⁶⁴ proposing that the 8 hour Rancimat induction time required for
410 European biodiesel is comparable to 27 minutes in a Petro-Oxy device, and the US standard
411 of 3 hours is comparable to 17 minutes of Petro-Oxy testing, where longer induction times
412 are indicative of higher oxidative stability. Due to limited equipment availability, only a
413 subset of OMEs were tested in this device, focusing primarily on larger alkyl groups (E-1-E,
414 P-1-P, P-2-P, B-1-B, B-2-B, B-3-B, iP-1-iP, and iB-1-iB). These were blended at 20 vol% in
415 tridecane to simulate common blending ratios in diesel and allow for higher resolution due
416 to lower concentrations of OME. The induction times for the tests are presented in Table
417 10. GC-MS testing was performed on the oxidized sample to determine the products of
418 the auto-oxidation reaction. Common products included alkyl esters, carboxylic acids, and

419 alcohols. The presence of carboxylic acids indicates that Rancimat tests may be effective for
 420 heavier OMEs which can survive the heated open system environment without significant
 421 vapor loss.

Table 10: Induction times of select OMEs in Petro-Oxy test, 20 vol% in tridecane

End Group	Number of CH ₂ O Units		
	1	2	3
Ethyl	228 min		
Propyl	86 min	91 min	
Butyl	106 min	152 min	174 min
Isopropyl	38 min		
Isobutyl	88 min		
Tridecane	154 min		

422 A trend is observed with the oxymethylene chain length; longer chains lead to improved
 423 stability. However, no clear trend can be seen for alkyl groups – E-1-E is more stable than
 424 any of the propyl or butyl OMEs, however, all of the butyl OMEs are more stable than
 425 the propyl ones. The iso-alkyl OMEs do show significantly reduced stability in comparison
 426 to their linear counterparts. The mechanisms by which this is occurring are unclear and
 427 warrant further investigation. All of the tested OMEs, in 20% blends, exceed the biodiesel
 428 oxidative stability standards, but it is unclear whether these fuels will exhibit stability issues
 429 when tested neat. Single tests were performed for each fuel, and so we refer to the ASTM
 430 standard, section 14.1.5,³⁸ where the reproducibility R of this method can be calculated as
 431 $R = 0.0863X + 1.3772$, to estimate an average R of 10% of the measured values.

432 Water Solubility

433 Water interaction with fuels is important for a number of reasons, but most importantly,
 434 there are environmental and combustion concerns. A fuel which is highly soluble in water

435 poses risks in case of spillage; it will be significantly harder to separate from water sources due
 436 to lack of distinct phases, and there is a risk of fuel becoming dissolved into groundwater in
 437 high concentrations and being spread from the spill site. Further, a fuel which can carry high
 438 concentrations of water dissolved in the fuel itself, while less of an environmental concern,
 439 poses risks to engine and fuel system operation and can reduce the effective LHV of the fuel.

Table 11: Water solubility of various OMEs [g OME / kg water]

End Group	Number of CH ₂ O Units				
	1	2	3	4	5
Methyl	481	469	394	338	283
Ethyl	56.0	60.7	52.3		
Propyl	3.16	3.72	3.23		
Butyl	0.215	0.189	0.251		
Isopropyl	9.76				
Isobutyl	6.62				
Typical Diesel	<0.1				

440 As shown in Table 11, the effect of additional oxymethylene units on the water solubility
 441 is negligible compared to the alkyl group effect, where increasing the alkyl group by one
 442 carbon per side reduces water solubility by roughly an order of magnitude each time. The
 443 mean CoV of these data is 6.9%, with B-3-B having the highest CoV at 19%. All of the
 444 B-n-B fuels exhibited high CoV due to measurable amounts of the fuels being only one order
 445 of magnitude greater the resolution of the balance used. Of the various properties tested,
 446 this one makes one of the strongest cases for the suitability of extended-alkyl (particularly
 447 butyl) OMEs for diesel blending. One anomaly is the behavior of iB-1-iB – while iP-1-iP is
 448 slightly higher than P-1-P, but within the same order of magnitude, iB-1-iB is an order of
 449 magnitude higher in water solubility than B-1-B. This result was sufficiently surprising that
 450 the entire series of iB-1-iB was retested with fresh samples, and the same result was found.

451 It is currently unclear what the chemical basis for this significant difference is, and more
452 investigation is warranted.

453 **Boiling Temperature**

454 Boiling temperatures were measured as a necessary result of the distillation process for
455 purification. Distillation was generally performed under vacuum (150 torr, 100 torr, or 30
456 torr, depending on the lightest component) except for when M-1-M was expected to be
457 present. The equivalent temperature at standard conditions (AET) was calculated using
458 the procedure in ASTM D1160 Appendix A7,⁴³ assuming a K factor of 12 (this value is
459 recommended in the standard unless another value can be clearly established) and using
460 units of torr and °C. A pressure correction A is first calculated from the distillation pressure
461 P , a temperature correction Δt from K and the pressure P , and then the AET calculated
462 from A , T , and Δt :

$$\Delta t = -1.4(K - 12)\log_{10}\left(\frac{760}{P}\right) \quad (4)$$

$$A = \frac{5.994295 - 0.972546\log_{10}P}{2663.129 - 95.76\log_{10}P} \quad (5)$$

$$AET = \frac{748.1A}{(T + 273.15)^{-1} + 0.3861A - 0.00051606} - 273.15 + \Delta t \quad (6)$$

463 The most likely source of error in these measurements is not from average boiling tem-
464 peratures observed at reduced pressure, which were typically within +/- 1°C, but rather the
465 uncertainty of the K factor. This is recommended in the standard as 12, but differing behav-
466 ior of OMEs from typical distillate fuels may require a different K value. As an example, a
467 +/-2 difference in K produces (at 30 and 150 torr reduced pressures, respectively) +/-3.93°C
468 and +/-1.97°C differences (where higher K leads to lower calculated temperature).

Table 12: Boiling temperature of various OMEs [°C]

End Group	Number of CH ₂ O Units				
	1	2	3	4	5
Methyl	42	112	161	207	243
Ethyl	88	142	186		
Propyl	141	184	223		
Butyl	179	223	257		
Isopropyl	119				
Isobutyl	164				
Typical Diesel (T10)	200				

469 The 10% distillation and 50% distillation temperatures (T10 and T50) of diesel fuel vary
 470 based on the specific blend but are often around 200°C and 250°C, respectively.⁴⁷ From the
 471 data in Table 12, it is clear that most of the tested OMEs are more volatile than even the
 472 low distillation components of a diesel; the only OMEs tested with boiling temperatures
 473 above T10 are M-4-M, M-5-M, P-3-P, B-2-B, and B-3-B, and only one tested OME (B-3-
 474 B) has a boiling temperature comparable to diesel T50. Consequently, diesels with OME
 475 components may experience preferential vaporization effects; effects of this on the combustion
 476 characteristics of diesel sprays is worthy of investigation.

477 **Material Compatibility**

478 Due to high required volumes of fuel for the material compatibility, this testing was performed
 479 only on a subset of OMEs with n=1. The effect of various chain lengths of M-n-M has been
 480 documented in literature,^{8,11,12} so this work focuses on the end group effect. Additionally,
 481 there is a wide range of possible sealant materials, and varying properties within categories of
 482 material, so it will be necessary for any engine development programs to do in-depth testing
 483 of the specifically selected materials. Thus, we present these data as being informative, but

484 not necessarily generalized.

485 The results of the material compatibility tests are provided in Figs. 10 and 11, where
486 the results are shown as mass increase due to fuel absorption (i.e. a 50% change represents
487 the material absorbing a mass of fuel equal to 50% of the original material), and thus the
488 desired result is to minimize this effect. The largest change in mass (due to fuel absorption)
489 occurred in the first 24 hours (Fig. 10), and equilibrium was reached by 72 hours (Fig. 11)
490 for all fuels and materials. For most, the change from the first measurement to equilibrium
491 was negligible; only FKM and NBR in M-1-M, silicone in E-1-E, and FKM in iP-1-iP had
492 significant ($>5\%$ by mass) changes after 24 hours. These measurements are an average of 2
493 samples, where the average deviation from the mean is 1.6%, with iP-1-iP having the widest
494 variation at 5.5%.

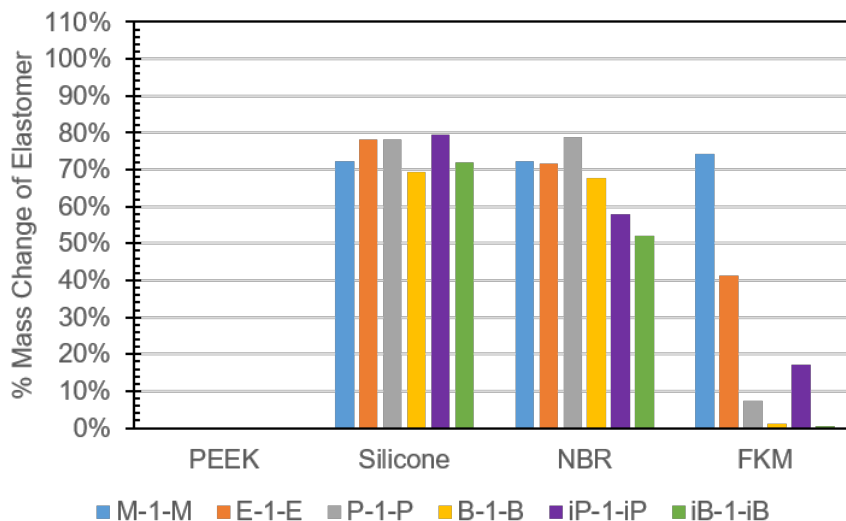


Figure 10: Percent change in mass of elastomer sample coupons after 24hr submerged exposure

495 One of the most important takeaways is the suitability of PEEK as a hard sealing or
496 handling material for OMEs; no absorption was observed for any of the tested OMEs at
497 any duration of exposure. For the elastomers, FKM was the only one which was suitable
498 for use with OMEs, and only for the extended alkyl OMEs – it has poor performance
499 for M-1-M, but shows significant reductions in mass of fuel absorbed as the alkyl group

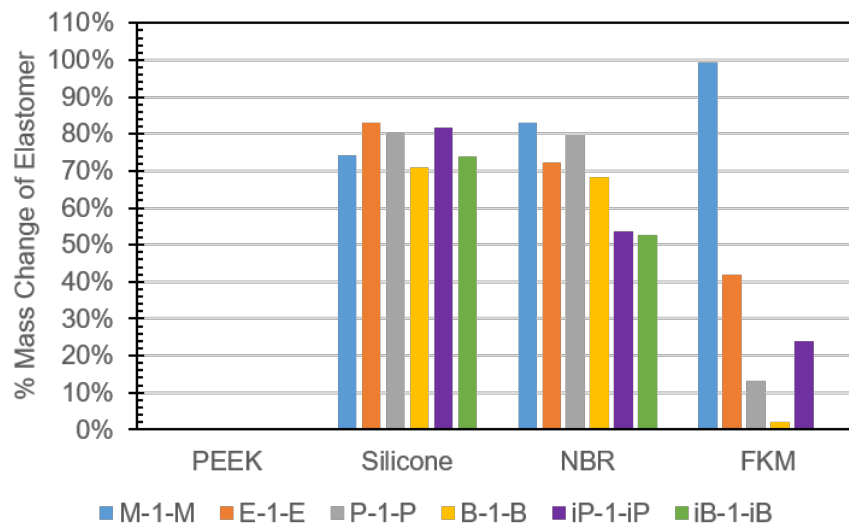


Figure 11: Percent change in mass of elastomer sample coupons after 72hr submerged exposure

500 is lengthened. Additionally, it is noted that the common trend observed in most other
 501 properties regarding the iso-OMEs, namely that they have somewhat inferior properties to
 502 their linear counterparts, does not hold here – iP-1-iP and iB-1-iB had less absorption than
 503 P-1-P and B-1-B for NBR samples, iB-1-iB less absorption than B-1-B in the FKM samples,
 504 and essentially comparable effects on silicone.

505 Conclusions

506 In this work, the properties of a wide array of OMEs are considered in the context of their
 507 suitability for use as diesel fuel blendstocks or substitutes. Methyl-terminated OMEs have
 508 been well studied with some attention given to ethyl-terminated OMEs, so the weaknesses
 509 of these fuels are well understood. Extending the range of possible OMEs to various propyl-
 510 and butyl-terminated OMEs allows a wider range of possible fuel properties and behaviors
 511 with which to balance the needs of any given application. Fig. 12 provides an overview of
 512 the trends in major properties with end group changes, with respect to diesel fuel.

513 In more detail, we observe the following trends in OME behaviors:

	Methyl	Ethyl	Propyl	Butyl	Isopropyl	Isobutyl
ICN	○	○	+	++	--	○
LHV	--	--	-	-	-	-
YSI	++	++	+	+	+	+
Water Solubility	--	--	-	○	-	-

++ = Significant improvement over diesel + = Improvement over diesel
 ○ = Comparable to diesel - = Inferior to diesel -- = Significantly inferior to diesel

Figure 12: Summary of trends in major properties with end groups, in comparison with diesel

- 514 • Most OMEs other than the lightest (M-1-M, E-1-E) and one branched version (iP-1-

515 iP) have suitable reactivity, as measured by ICN, and B-n-B OMEs show the most

516 consistent ICN with variance in central chain length.
- 517 • All OMEs have significant LHV reductions in comparison to diesel or even traditional

518 biodiesels. Shorter chains with longer alkyl groups provide the highest LHV.
- 519 • All OMEs show significant reductions in soot production compared to diesel. M-n-M

520 OMEs, the most commonly studied, retain the advantage here, but even the worst

521 OME has a 3.1x reduction of soot per unit energy compared to diesel fuels.
- 522 • Lighter OMEs have flash points too low to be suitable diesel blendstocks, however,

523 heavier OMEs in either chain length or alkyl group (MW > ~160) have acceptable flash

524 points.
- 525 • Shorter oligomers of OMEs have comparable densities to diesel, with longer oxymethy-

526 lene chains increasing density above typical diesel fuels. All OMEs have viscosities

527 lower than diesel standards, although heavier OMEs such as B-3-B and M-5-M ap-

528 proach diesel requirements.

- 529 • Many OMEs such as n=1 and methyl-terminated OMEs have high vapor pressure
530 compared to lighter diesel components such as dodecane.
- 531 • No clear trends are apparent in oxidative stability, however, at moderate blending
532 ratios in diesel, most OMEs appear to have acceptable stability.
- 533 • Water solubility is dominated by alkyl groups, where larger alkyl groups have order-
534 of-magnitude reductions in solubility. B-n-B shows the lowest solubility, on the order
535 of that observed for diesel fuel.
- 536 • Most OMEs have boiling temperatures below the typical T10 distillation temperature
537 of traditional diesel fuel.
- 538 • Common elastomers such as nitrile and silicone appear to be insensitive to alkyl groups
539 and will absorb n=1 OMEs equally, with significant absorption. FKM (“Viton”)
540 fluoroelastomers show improved resistance to OMEs with larger alkyl groups, par-
541 ticularly branched alkyl groups. PEEK is entirely unaffected by OMEs.

542 The choice of an ideal OME for future use as a CI fuel will be dependent on balancing the
543 various goals of the application. For example, an engine design focusing on maximizing soot
544 removal at all costs would be best served continuing to focus on methyl-terminated OMEs,
545 while a focus on maximum compatibility with current diesel fuels and their distribution
546 networks and fueling systems may be best served by considering heavier OMEs with longer
547 alkyl groups. Spark-ignited applications may consider use of iP-1-iP as a blendstock for
548 soot reduction, as it shows high autoignition resistance compared to many OMEs while
549 maintaining good soot reduction properties and higher LHV than ethanol, a common gasoline
550 oxygenate. In addition to their use as soot reduction fuels, OMEs have potential to be bio-
551 sourced, produced via e-fuel processes, or a combination thereof. Upcoming work is focusing
552 on the techno-economic analysis and life-cycle effects of the production of butyl-terminated
553 OMEs, which have multiple production pathways possible via bio-sources, and show promise

554 for reducing emissions while maintaining minimal gallon-equivalent costs. Further possible
555 areas of research include engine optimization studies of NO_x and soot emissions, wherein,
556 as a result of their naturally low propensity to soot, OMEs may be applied in low NO_x
557 engine operating strategies (e.g., high EGR) while maintaining manageable levels of soot, or
558 usage of OMEs as low-sooting option for the high-reactivity or prechamber fuel in dual-fuel
559 applications with low-soot fuels such as methanol. It is the hope of the authors that this
560 work will help jump-start additional research into a number of these unstudied and under-
561 studied OMEs and their possible future engine applications, where their unique properties
562 may aid in the reduction of emissions and life cycle environmental effects.

563 **Acknowledgement**

564 Funding for this research is provided in part by U.S. Department of Energy’s Office of Energy
565 Efficiency and Renewable Energy under the Bioenergy Technologies Office, Co-Optimization
566 of Fuels and Engines Initiative award number DE-EE0008726, and additional funding from
567 the Bioenergy Technologies Office under Contract Nos. DE-AC36-08GO28308 and DE347-
568 AC36-99GO10337. Additional financial support was provided by the Colorado Energy Re-
569 search Collaboratory. We thank Lambiotte & Cie for the donation of a sample of P-1-P.

570 **References**

- 571 (1) International Energy Agency, *The Future of Trucks*; 2017.
- 572 (2) Cunanan, C.; Tran, M.-K.; Lee, Y.; Kwok, S.; Leung, V.; Fowler, M. A Review of
573 Heavy-Duty Vehicle Powertrain Technologies: Diesel Engine Vehicles, Battery Electric
574 Vehicles, and Hydrogen Fuel Cell Electric Vehicles. *Clean Technologies* **2021**, *3*, 474–
575 489.

- 576 (3) Williams, M.; Minjares, R. *A technical summary of Euro 6/VI vehicle emission stan-*
577 *dards*; 2016.
- 578 (4) Sorenson, S. C. Dimethyl Ether in Diesel Engines: Progress and Perspectives . *Journal*
579 *of Engineering for Gas Turbines and Power* **2000**, *123*, 652–658.
- 580 (5) Burger, J.; Siegert, M.; Ströfer, E.; Hasse, H. Poly(oxymethylene) dimethyl ethers as
581 components of tailored diesel fuel: Properties, synthesis and purification concepts. *Fuel*
582 **2010**, *89*, 3315–3319.
- 583 (6) Lütenschütz, L.; Oestreich, D.; Seidenspinner, P.; Arnold, U.; Dinjus, E.; Sauer, J.
584 Physico-chemical properties and fuel characteristics of oxymethylene dialkyl ethers.
585 *Fuel* **2016**, *173*, 129–137.
- 586 (7) Omari, A.; Heuser, B.; Pischinger, S.; Rüdinger, C. Potential of long-chain oxymethy-
587 lene ether and oxymethylene ether-diesel blends for ultra-low emission engines. *Applied*
588 *Energy* **2019**, *239*, 1242–1249.
- 589 (8) Pélerin, D.; Gaukel, K.; Härtl, M.; Jacob, E.; Wachtmeister, G. Potentials to simplify
590 the engine system using the alternative diesel fuels oxymethylene ether OME1 and
591 OME3-6 on a heavy-duty engine. *Fuel* **2020**, *259*, 116231.
- 592 (9) ASTM International, *ASTM D975-21 Standard Specification for Diesel Fuel*; 2021.
- 593 (10) European Committee for Standardization, *EN 590:2022 Automotive fuels - Diesel -*
594 *Requirements and test methods*; 2022.
- 595 (11) Schröder, J.; Görsch, K. Storage stability and material compatibility of poly (oxymethy-
596 lene) dimethyl ether diesel fuel. *Energy & Fuels* **2019**, *34*, 450–459.
- 597 (12) Kass, M.; Wissink, M.; Janke, C.; Connatser, R.; Curran, S. Compatibility of Elas-
598 tomers with Polyoxymethylene Dimethyl Ethers and Blends with Diesel. *SAE Interna-*
599 *tional Journal of Advances and Current Practices in Mobility* **2020**, *2*, 1963–1973.

- 600 (13) Kass, M.; Janke, C.; Nafziger, E. Impact of Biodiesel, Renewable Diesel, 1-Octanol,
601 Dibutoxymethane, n-Undecane, Hexyl hexanoate and 2-Nonanone with Infrastructure
602 Plastics as Blends with Diesel. WCX SAE World Congress Experience. 2022.
- 603 (14) Bartholet, D. L.; Arellano-Treviño, M. A.; Chan, F. L.; Lucas, S.; Zhu, J.; St.
604 John, P. C.; Alleman, T. L.; McEnally, C. S.; Pfefferle, L. D.; Ruddy, D. A.; Win-
605 dom, B.; Foust, T. D.; Reardon, K. F. Property predictions demonstrate that struc-
606 tural diversity can improve the performance of polyoxymethylene ethers as potential
607 bio-based diesel fuels. *Fuel* **2021**, *295*, 120509.
- 608 (15) Lehrheuer, B.; Hoppe, F.; Heufer, K. A.; Jacobs, S.; Minwegen, H.; Klankermayer, J.;
609 Heuser, B.; Pischinger, S. Diethoxymethane as tailor-made fuel for gasoline controlled
610 autoignition. *Proceedings of the Combustion Institute* **2019**, *37*, 4691–4698.
- 611 (16) Kröger, L. C.; Döntgen, M.; Firaha, D.; Kopp, W. A.; Leonhard, K. Ab initio kinetics
612 predictions for H-atom abstraction from diethoxymethane by hydrogen, methyl, and
613 ethyl radicals and the subsequent unimolecular reactions. *Proceedings of the Combustion*
614 *Institute* **2019**, *37*, 275–282.
- 615 (17) Li, R.; Herreros, J. M.; Tsolakis, A.; Yang, W. Chemical kinetic modeling of di-
616 ethoxymethane oxidation: A carbon-neutral fuel. *Fuel* **2021**, *291*, 120217.
- 617 (18) Jacobs, S.; Döntgen, M.; Alqaity, A. B. S.; Hesse, R.; Kruse, S.; Beeckmann, J.;
618 Kröger, L. C.; Morsch, P.; Leonhard, K.; Pitsch, H.; Heufer, K. A. A Comprehen-
619 sive Experimental and Kinetic Modeling Study of the Combustion Chemistry of Di-
620 ethoxymethane. *Energy & Fuels* **2021**, *35*, 16086–16100.
- 621 (19) Drexler, M.; Haltenort, P.; Zevaco, T. A.; Arnold, U.; Sauer, J. Synthesis of tailored
622 oxymethylene ether (OME) fuels via transacetalization reactions. *Sustainable Energy*
623 *& Fuels* **2021**, *5*, 4311–4326.

- 624 (20) Murphy, M. J. Oxygenate compatibility with diesel fuels. *SAE Transactions* **2002**,
625 1864–1870.
- 626 (21) Arellano-Treviño, M. A. et al. Synthesis of Butyl-Exchanged Polyoxymethylene Ethers
627 as Renewable Diesel Blendstocks with Improved Fuel Properties. *ACS Sustainable*
628 *Chemistry & Engineering* **2021**, *9*, 6266–6273.
- 629 (22) An, G.; Xia, Y.; Xue, Z.; Shang, H.; Cui, S.; Lu, C. Combination of Theoretical and
630 Experimental Insights into the Oxygenated Fuel Poly(oxymethylene) Dibutyl Ether
631 from n-Butanol and Paraformaldehyde. *ACS Omega* **2022**, *7*, 3064–3072.
- 632 (23) Haltenort, P.; Hackbarth, K.; Oestreich, D.; Lautenschütz, L.; Arnold, U.; Sauer, J.
633 Heterogeneously catalyzed synthesis of oxymethylene dimethyl ethers (OME) from
634 dimethyl ether and trioxane. *Catalysis Communications* **2018**, *109*, 80–84.
- 635 (24) Breitzkreuz, C. F.; Schmitz, N.; Ströfer, E.; Burger, J.; Hasse, H. Design of a Production
636 Process for Poly(oxymethylene) Dimethyl Ethers from Dimethyl Ether and Trioxane.
637 *Chemie Ingenieur Technik* **2018**, *90*, 1489–1496.
- 638 (25) To, A. T.; Wilke, T. J.; Nelson, E.; Nash, C. P.; Bartling, A.; Wegener, E. C.; Un-
639 ocic, K. A.; Habas, S. E.; Foust, T. D.; Ruddy, D. A. Dehydrogenative Coupling of
640 Methanol for the Gas-Phase, One-Step Synthesis of Dimethoxymethane over Supported
641 Copper Catalysts. *ACS Sustainable Chemistry & Engineering* **2020**, *8*, 12151–12160.
- 642 (26) Baranowski, C. J.; Bahmanpour, A. M.; Kröcher, O. Catalytic synthesis of poly-
643 oxymethylene dimethyl ethers (OME): A review. *Applied Catalysis B: Environmental*
644 **2017**, *217*, 407–420.
- 645 (27) Gautam, P.; Neha,; Upadhyay, S.; Dubey, S. Bio-methanol as a renewable fuel from
646 waste biomass: Current trends and future perspective. *Fuel* **2020**, *273*, 117783.

- 647 (28) Ndaba, B.; Chiyanzu, I.; Marx, S. n-Butanol derived from biochemical and chemical
648 routes: A review. *Biotechnology Reports* **2015**, *8*, 1–9.
- 649 (29) Thavornprasert, K.-a.; Capron, M.; Jalowiecki-Duhamel, L.; Dumeignil, F. One-pot 1,
650 1-dimethoxymethane synthesis from methanol: a promising pathway over bifunctional
651 catalysts. *Catalysis Science & Technology* **2016**, *6*, 958–970.
- 652 (30) Härtl, M.; Seidenspinner, P.; Jacob, E.; Wachtmeister, G. Oxygenate screening on a
653 heavy-duty diesel engine and emission characteristics of highly oxygenated oxymethy-
654 lene ether fuel OME1. *Fuel* **2015**, *153*, 328–335.
- 655 (31) Deutsch, D.; Oestreich, D.; Lautenschütz, L.; Haltenort, P.; Arnold, U.; Sauer, J. High
656 purity oligomeric oxymethylene ethers as diesel fuels. *Chemie Ingenieur Technik* **2017**,
657 *89*, 486–489.
- 658 (32) ASTM International, *ASTM D8183-18 Standard Test Method for Determination of In-*
659 *dicated Cetane Number (ICN) of Diesel Fuel Oils using a Constant Volume Combustion*
660 *Chamber—Reference Fuels Calibration Method*; 2018.
- 661 (33) Abel, R. C.; Luecke, J.; Ratcliff, M. A.; Zigler, B. T. Comparing Cetane Number
662 Measurement Methods. 2020; V001T02A009.
- 663 (34) ASTM International, *ASTM D240-19 Standard Test Method for Heat of Combustion*
664 *of Liquid Hydrocarbon Fuels by Bomb Calorimeter*; 2019.
- 665 (35) ASTM International, *ASTM D93-20 Standard Test Methods for Flash Point by Pensky-*
666 *Martens Closed Cup Tester*; 2020.
- 667 (36) ASTM International, *ASTM D7042-21a Standard Test Method for Dynamic Viscosity*
668 *and Density of Liquids by Stabinger Viscometer (and the Calculation of Kinematic*
669 *Viscosity)*; 2021.

- 670 (37) ASTM International, *ASTM D6378-20 Standard Test Method for Determination of Va-*
671 *por Pressure (VPX) of Petroleum Products, Hydrocarbons, and Hydrocarbon-Oxygenate*
672 *Mixtures (Triple Expansion Method)*; 2020.
- 673 (38) ASTM International, *ASTM D7545-14(2019)e1 Standard Test Method for Oxidation*
674 *Stability of Middle Distillate Fuels—Rapid Small Scale Oxidation Test (RSSOT)*; 2019.
- 675 (39) McEnally, C. S.; Pfefferle, L. D. Improved sooting tendency measurements for aromatic
676 hydrocarbons and their implications for naphthalene formation pathways. *Combustion*
677 *and Flame* **2007**, *148*, 210–222.
- 678 (40) Montgomery, M. J.; Das, D. D.; McEnally, C. S.; Pfefferle, L. D. Analyzing the robust-
679 ness of the yield sooting index as a measure of sooting tendency. *Proceedings of the*
680 *Combustion Institute* **2019**, *37*, 911–918.
- 681 (41) McEnally, C. S.; Xuan, Y.; John, P. C. S.; Das, D. D.; Jain, A.; Kim, S.; Kwan, T. A.;
682 Tan, L. K.; Zhu, J.; Pfefferle, L. D. Sooting tendencies of co-optima test gasolines and
683 their surrogates. *Proceedings of the Combustion Institute* **2019**, *37*, 961–968.
- 684 (42) Zhu, J.; Chan, F. L.; Foust, T. D.; Lucas, S.; Montgomery, L. D., M. J. and Pfefferle;
685 Reardon, K. F.; Windom, B. C.; McEnally, C. S. Poly(oxymethylene) Ethers: Potential
686 Diesel Fuels with Low Sooting Tendencies. 2020 Virtual AIChE Annual Meeting. 2021.
- 687 (43) ASTM International, *ASTM D1160-18 Standard Test Method for Distillation of*
688 *Petroleum Products at Reduced Pressure*; 2018.
- 689 (44) Lucas, S. P.; Labbe, N. J.; Marchese, A. J.; Windom, B. Pre-Vaporized Ignition Behav-
690 ior of Ethyl- and Propyl-Terminated Oxymethylene Ethers. *Proceedings of the Com-*
691 *bustion Institute* **2022**, *39*.
- 692 (45) Yanowitz, J.; Ratcliff, M. A.; McCormick, R. L.; Taylor, J. D.; Murphy, M. J. *Com-*
693 *pendium of Experimental Cetane Numbers*; 2017.

- 694 (46) Nicolle, A.; Naser, N.; Javed, T.; Rankovic, N.; Sarathy, S. M. Autoignition characteris-
695 tics of ethers blended with low cetane distillates. *Energy & Fuels* **2019**, *33*, 6775–6787.
- 696 (47) Lopes, S. M.; Furey, R.; Geng, P. Calculation of heating value for diesel fuels containing
697 biodiesel. *SAE International Journal of Fuels and Lubricants* **2013**, *6*, 407–418.
- 698 (48) Gülüm, M.; Bilgin, A. Density, flash point and heating value variations of corn oil
699 biodiesel–diesel fuel blends. *Fuel Processing Technology* **2015**, *134*, 456–464.
- 700 (49) Bezergianni, S.; Dimitriadis, A. Comparison between different types of renewable diesel.
701 *Renewable and Sustainable Energy Reviews* **2013**, *21*, 110–116.
- 702 (50) McAllister, S.; Chen, J.-Y.; Fernandez-Pello, A. C. *Fundamentals of combustion pro-*
703 *cesses*; Springer, 2011; Vol. 302.
- 704 (51) Tan, Y. R.; Botero, M. L.; Sheng, Y.; Dreyer, J. A.; Xu, R.; Yang, W.; Kraft, M. Sooting
705 characteristics of polyoxymethylene dimethyl ether blends with diesel in a diffusion
706 flame. *Fuel* **2018**, *224*, 499–506.
- 707 (52) Cho, C. H.; Han, K. R.; Sohn, C. H.; Haas, F. M. Sooting Propensity Estimation of Jet
708 Aviation Fuel Surrogates and Their n-Alkane Components by the Virtual Smoke Point
709 Method. *Energy & Fuels* **2020**, *34*, 15072–15076.
- 710 (53) National Fire Protection Association, *NFPA 30 Flammable and Combustible Liquids*
711 *Code*; 2020.
- 712 (54) Lefebvre, A. H.; McDonell, V. G. *Atomization and sprays*; CRC press, 2017.
- 713 (55) Algayyim, S. J. M.; Wandel, A. P. Macroscopic and microscopic characteristics of biofuel
714 spray (biodiesel and alcohols) in CI engines: A review. *Fuel* **2021**, *292*, 120303.
- 715 (56) Hayashi, J.; Watanabe, H.; Kurose, R.; Akamatsu, F. Effects of fuel droplet size on
716 soot formation in spray flames formed in a laminar counterflow. *Combustion and Flame*
717 **2011**, *158*, 2559–2568.

- 718 (57) National Institute of Standards and Technology, Methylal Phase change data.
719 [https://webbook.nist.gov/cgi/cbook.cgi?ID=C109875&Units=SI&](https://webbook.nist.gov/cgi/cbook.cgi?ID=C109875&Units=SI&Mask=4#Thermo-Phase)
720 [Mask=4#Thermo-Phase](https://webbook.nist.gov/cgi/cbook.cgi?ID=C109875&Units=SI&Mask=4#Thermo-Phase), Accessed 2022-03-09.
- 721 (58) National Institute of Standards and Technology, Methane, diethoxy- Phase change
722 data. [https://webbook.nist.gov/cgi/cbook.cgi?ID=C462953&Units=SI&Mask=4#](https://webbook.nist.gov/cgi/cbook.cgi?ID=C462953&Units=SI&Mask=4#Thermo-Phase)
723 [Thermo-Phase](https://webbook.nist.gov/cgi/cbook.cgi?ID=C462953&Units=SI&Mask=4#Thermo-Phase), Accessed 2022-03-09.
- 724 (59) National Institute of Standards and Technology, Heptane Phase change data. [https://](https://webbook.nist.gov/cgi/cbook.cgi?ID=C142825&Units=SI&Mask=4#Thermo-Phase)
725 webbook.nist.gov/cgi/cbook.cgi?ID=C142825&Units=SI&Mask=4#Thermo-Phase,
726 Accessed 2022-03-09.
- 727 (60) National Institute of Standards and Technology, Decane Phase change data. [https://](https://webbook.nist.gov/cgi/cbook.cgi?ID=C124185&Units=SI&Mask=4#Thermo-Phase)
728 webbook.nist.gov/cgi/cbook.cgi?ID=C124185&Units=SI&Mask=4#Thermo-Phase,
729 Accessed 2022-03-09.
- 730 (61) National Institute of Standards and Technology, Dodecane Phase change
731 data. [https://webbook.nist.gov/cgi/cbook.cgi?ID=C112403&Units=SI&Mask=4#](https://webbook.nist.gov/cgi/cbook.cgi?ID=C112403&Units=SI&Mask=4#Thermo-Phase)
732 [Thermo-Phase](https://webbook.nist.gov/cgi/cbook.cgi?ID=C112403&Units=SI&Mask=4#Thermo-Phase), Accessed 2022-03-09.
- 733 (62) Focke, W. W.; Van der Westhuizen, I.; Oosthuysen, X. Biodiesel oxidative stability
734 from Rancimat data. *Thermochimica Acta* **2016**, *633*, 116–121.
- 735 (63) Alves-Fortunato, M.; Baroni, A.; Neocel, L.; Chardin, M.; Matrat, M.; Boucaud, C.;
736 Mazarin, M. Gasoline Oxidation Stability: Deposit Formation Tendencies Evaluated by
737 PetroOxy and Autoclave Methods and GDI/PFI Engine Tests. *Energy & Fuels* **2021**,
738 *35*, 18430–18440.
- 739 (64) Botella, L.; Bimbela, F.; Martín, L.; Arauzo, J.; Sánchez, J. L. Oxidation stability
740 of biodiesel fuels and blends using the Rancimat and PetroOXY methods. Effect of
741 4-allyl-2, 6-dimethoxyphenol and catechol as biodiesel additives on oxidation stability.
742 *Frontiers in chemistry* **2014**, *2*, 43.

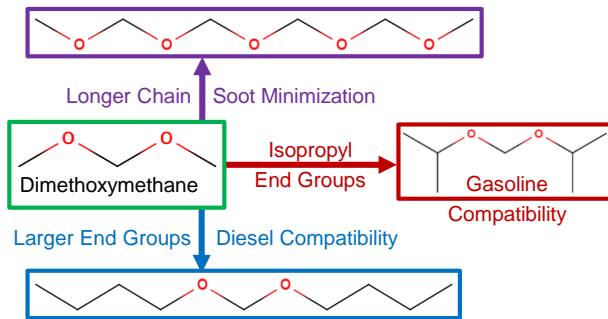


Table of Contents (TOC)/Abstract Graphic